International Journal of Nanomedicine

Dovepress
open access to scientific and medical research

Open Access Full Text Article

ORIGINAL RESEARCH

A Novel Airway-Organoid Model Based on a Nano-Self-Assembling Peptide: Construction and Application in Adenovirus Infection Studies

Yun-E Xu[1,*], Di-Shu Ao[1,*], Xin Sun[1], Wei Chen[2], Xue Luo[1], Can Zhao[1], Sheng-Yu Wang[1], Hong Song[1]

[1]Department of Microbiology, School of Basic Medical Sciences, Zunyi Medical University, Zunyi, 563000, People's Republic of China; [2]Department of Hepatobiliary Surgery, Third Affiliated Hospital of Zunyi Medical University (The First People's Hospital of Zunyi), Zunyi, 563000, People's Republic of China

*These authors contributed equally to this work

Correspondence: Hong Song, Department of Microbiology, School of Basic Medical Sciences, Zunyi Medical University, Zunyi, 563000, People's Republic of China, Tel +86-18985259977; +86-0851-28643582, Email hongsong@zmu.edu.cn

Purpose: Hydrogels containing the nano-self-assembling peptide RADA16-I (Nanogels) were utilized as scaffolds to establish airway organoids and an adenovirus-infected model. The results support in vitro adenovirus studies, including isolation and culture, pathogenesis research, and antiviral drug screening.

Methods: HSAEC1-KT, HuLEC-5a and HELF cells were cocultured in RADA16-I hydrogel scaffolds to construct an airway organoid model. Adenovirus was used to infect this model for adenovirus-related studies. The morphological characteristics and the proliferation and activity of airway organoids before and after adenovirus infection were evaluated. The expression of the airway organoid marker proteins CC10, KRT8, AQP5, SPC, VIM and CD31 was detected. TEM and qPCR were used to detect adenovirus proliferation in airway organoids.

Results: HSAEC1-KT, HuLEC-5a and HELF cells cocultured at 10:7:2 self-assembled into airway organoids and maintained long-term proliferation in a RADA16-I hydrogel 3D culture system. The organoids stably expressed the lumen-forming protein KRT8 and the terminal airway markers AQP5 and SPC. Adenoviruses maintained long-term proliferation in this model.

Conclusion: An airway-organoid model of adenovirus infection was constructed in vitro from three human lung-derived cell lines on RADA16-I hydrogels. The model has potential as a novel research tool for adenovirus isolation and culture, pathogenesis research, and antiviral drug screening.

Keywords: nano-self-assembling peptide, RADA16-I hydrogels, airway organoids, adenovirus

Introduction

Viral diseases are important among diseases caused by pathogenic microorganisms, which seriously endanger human health and threaten human life. However, there is not enough research on the human infection and replication processes of viruses, virus and host interactions, host antiviral immune responses, etc., which restricts the research and development of antiviral drugs. Current research on a variety of human viral diseases and antiviral drugs is based primarily on the use of traditional two-dimensional (2D) monolayer cell culture or animal models. However, 2D monolayer cell culture cannot accurately mimic the physiological conditions of the in vivo microenvironment in humans, and it cannot accurately reproduce the natural infection process or the host's response. Moreover, animal models are expensive, and there are ethical problems related to their use. There are species differences between animals and humans, and viral pathogenesis in humans typically cannot be captured or simulated in animal models.[1] With the development of biotechnology, three-dimensional (3D) cell culture technology based on cell scaffolds has been developed and can simulate the physiological conditions of natural organs.[2] Some scholars have applied various types of 3D cell culture

Received: 23 April 2023
Accepted: 28 August 2023
Published: 13 September 2023

models to viral cell culture in vitro,[3–7] and studies have found that some viruses that cannot proliferate in traditional 2D cell culture models, such as human rhinovirus and human Boca virus, can proliferate in 3D cell culture.[8] However, organs and tissues in vivo are composed of many kinds of cells. The local microenvironment of virus invasion is formed by the interaction between cells and the extracellular matrix. Therefore, the virus infection model constructed by a single type of cell still has some limitations.

Organoids are 3D structures formed by the self-assembly of human embryonic stem cells (hESCs), human induced pluripotent stem cells (hiPSCs), human adult stem cells (hASCs) or a variety of other cell lines in vitro.[9–14] As the cell composition, tissue organization, physiological characteristics, and even functions are similar to those of natural organs in the body, these organoids simulate the physiological state of body tissues to the greatest extent, so they can more truly reflect the occurrence and development of body physiology and pathophysiology. Recent studies have shown that organoid culture is a powerful tool for research on human viruses, including respiratory viruses, enteroviruses, and neuroviruses.[6,15–18] Organoid culture requires cell growth scaffolds to provide a spatial framework. Matrigel et al are currently the most popular cell scaffolds. However, these kinds of scaffold materials come from animals, and maintaining a consistent composition across batches is difficult; there may also be potential pathogens.[19] These factors may interfere with the experimental results. Nano-self-assembling peptide RADA16-I (Ac-RADARADARADA-CONH2) is a chemically synthesized biomaterial. It has unique amino acid sequences and can self-assemble into nanofiber hydrogels with more than 99% water content in physiological saline solutions.[20] Their porosity and high water content are conducive not only to cell adhesion and growth but also to the diffusion and absorption of various nutrients and signal molecules in the microenvironment.[21] Compared with natural cell culture scaffold materials, RADA16-I hydrogels have stable ingredients, display no immunogenicity, no dangerous pathogens, and no cytotoxicity and can promote cell adhesion, growth and differentiation. At present, RADA16-I and its derivatives are undergoing increasingly extensive research and application in cell culture, tissue engineering, regenerative medicine and other fields.[22,23]

In previous studies, RADA16-I hydrogels were successfully used for different mammalian cell cultures, including chondrocytes, liver cancer cells, ovarian cancer cells, and 293T cells.[24–27] The cells grew as microspheres, and their proliferation activity was similar to that in Matrigel et al.[26] We also successfully constructed a 3D culture model of adenovirus in vitro. Research has shown that adenovirus can continue to proliferate in a 3D culture model.[27,28] However, viral infection in vivo is a complex process, and the target organ of infection is often composed of a variety of cells. Respiratory bronchioles originate from the endoderm and are the target organ of adenovirus infection. They consist mainly of airway epithelial cells, mesenchymal cells and vascular endothelial cells. To further simulate the real microenvironment of adenovirus survival in vivo, this study used human small airway epithelial cells (HSAEC1-KT), human lung microvascular endothelial cells (HuLEC-5a) and human embryonic lung fibroblasts (HELF) to construct an airway-organoid model for adenovirus infection using RADA16-I Nanogel as a culture scaffold in vitro, providing an experimental tool for virus isolation and culture, pathogenesis research, and antiviral drug screening and providing an experimental and theoretical basis for the application of this kind of chemically synthesized nano self-assembled short peptide in virology research.

Materials and Methods

Materials

HSAEC1-KT and HuLEC-5a cells were purchased from Shanghai BinSui Biological Technology Co., Ltd. (Shanghai, China). The HELF cell line was purchased from CCTCC (Wuhan Province, China). Adenovirus-EGFP was purchased from Shanghai GeneChem Co., Ltd. (Shanghai, China). Dulbecco's modified Eagle's medium Nutrient Mixture F-12 (catalog No. 8120317) and fetal bovine serum (catalog No. 10099141) were purchased from Gibco (USA). MTS (catalog No. 0000277301) was purchased from Promega (USA). Calcein-AM (Ca-AM, catalog No. C0875), phalloidin (catalog No. P5282), propidium iodide (PI, catalog No. C0080), 4′6-diamidino-2-phenylindole (DAPI, catalog No. C0065), and a DNA Quantitation Kit (catalog No. DNAQF) were purchased from Sigma–Aldrich (USA). Primary antibodies against CC10 (catalog No. 49757), VIM (catalog No. 21488), CD31 (catalog No. 29555), AQP5 (catalog No. 29573), SPC (catalog No. C32459) and KRT8 (catalog No. 38010) and secondary antibodies against AF488-labeled goat anti-mouse

IgG (catalog No. L3016) and AF647-labeled goat anti-rabbit IgG (catalog No. L3038) were purchased from Signalway Antibody LLC (USA). The TIANamp Virus DNA/RNA Kit was purchased from Tiangen Biochemical Technology Co., Ltd. (catalog No. DP315, Beijing, China). qPCR primers were purchased from Thermo Fisher Scientific (USA). The nano-self-assembling peptide RADA16-I (Ac-RADA RADA RADARADA-CONH2, purity 99%) was synthesized by Shanghai Biotech Bioscience & Technology Co., Ltd. (catalog No. pep20201109-91, Shanghai, China).

Material Characterization

The RADA16-I hydrogel was prepared to 0.5% weight/volume (wt/vol) and washed. The 0.5% RADA16-I hydrogel was fixed with 2.5% (v/v) glutaraldehyde for 2 h at 37°C and dehydrated in 70%, 80%, 90%, and 100% ethanol. Critical point drying was used to dry the samples. Finally, the samples were mounted on scanning electron microscopy (SEM) stubs using double-coated carbon-conductive tape for SEM (Hitachi, S-3400 N, Japan) observation.

Generation of Human Airway Organoids

3D Cell Culture

HSAEC1-KT, HuLEC-5a and HELF cells were seeded in 25-cm^2 culture flasks and grown at 37°C in a humidified atmosphere containing 5% CO_2 in DMEM/F-12 supplemented with 10% fetal calf serum. When the density reached 90%, each tape of cells was detached using 0.05% trypsin-EDTA and washed twice with a 10% sucrose solution. The density of each of the three sucrose cell suspensions was adjusted to 4×10^5/mL. The ratio of the HSAEC1-KT: HuLEC-5a: HELF cell types was 10:7:2. Twenty-five microliters of a cell suspension containing 1×10^4 cells was added to 25 μL of 1% RADA16-I hydrogel (HSAEC1-KT, HuLEC-5a, HELF cells and a mixture of these cells at 10:7:2 were inoculated according to this inoculation method), gently mixed, and deposited in a 12-well plate with complete medium. Each well was inoculated with 3 gel-cell clumps and incubated at 37°C with 5% CO_2 for 30 min before the first medium change. Twenty-four hours later, the medium was changed again. Afterward, the medium was changed at 1-day intervals. For some experiments, 3D cultures were scaled to a 96-well plate using 25 μL of cell suspension containing 1×10^4 cells and 25 μL of 1% RADA16-I hydrogel, and each hole was inoculated with 1 gel-cell clump.

Morphological and Histological Observation

To test anchorage-dependent cell growth in RADA16-I hydrogels, 3D-cultivated cells were incubated in 12-well plates, and the morphology was observed using inverted phase contrast microscopy, SEM and transmission electron microscopy (TEM). For SEM measurements, airway organoids were cultured in RADA16-I hydrogels for 7 days, washed with PBS twice, fixed with 2.5% (v/v) glutaraldehyde for 2 h at 37°C, and dehydrated in 70%, 80%, 90%, and 100% ethanol. Critical point drying was used to dry the samples. Finally, the samples were mounted on SEM stubs using double-coated carbon-conductive tape for SEM observation. For TEM, the airway organoids were harvested at 7 days. Afterward, the samples were postfixed using 1% osmic acid at 4°C for 3 h, dehydrated through a graded series of alcohol, embedded with Spurr resin, and cut into ultrathin sections (thickness 70 nm). Specimens were then stained with uranyl acetate and lead citrate, and images were obtained using a JEM1230 TEM (JEOL, Japan) at an acceleration voltage of 80 kV.

The airway organoids were cultured in RADA16-I hydrogels for 14 days and then embedded in optimal cutting temperature (OCT) compound. For HE staining, 10 μm longitudinal sections were stained with hematoxylin solution for 5 min followed by 5 s in 1% acid ethanol and then rinsed in distilled water. Then, the sections were stained with eosin solution for 5 min followed by dehydration with graded alcohol. For phalloidin/DAPI staining, 10 μm longitudinal sections were fixed with 4% paraformaldehyde and washed with PBS twice. The gel-cell clumps were then permeabilized with PBS containing 0.3% Triton X-100 for 20 min, stained for 5 min with rhodamine phalloidin (Invitrogen) and DAPI, and washed with PBS buffer. The mounted slides were then examined and photographed using an Olympus IX71 fluorescence microscope. The morphological and structural characteristics of airway organoids were observed by H&E and phalloidin staining. The morphological and structural characteristics of human lung tissue were observed as a control.

Cell Viability and Cell Proliferation

3D-cultivated cells and airway organoids were incubated in 96-well plates, and 20 μL of MTS reagent was added directly to the wells at 0, 4, 8…, and 20 days after cultivation. Then, the cell samples were incubated at 37°C for 2 h in the dark, and the absorbance was measured at 490 nm. 3D-cultivated cells and airway organoids were incubated in 96-well plates and collected at 0, 4, 8…, and 20 days after cultivation. The DNA density (μg/mL) was determined by fluorometric quantification of the DNA content using a DNA fluorescence assay kit according to the manufacturer's instructions (Invitrogen, molecular probes). For qualitative observations of cell proliferation, the gel-cell clumps were incubated in PBS containing 1.2 μg/mL calcein AM to stain the live cells, and 10 μg/mL propidium iodide (PI) was used to stain dead cells. An inverted Olympus IX71 fluorescence microscope was used to capture fluorescent signals.

Immunofluorescence Staining

Fresh RADA16-I hydrogel 3D airway organoid cultures and adult human lung tissues were embedded in optimal cutting temperature (OCT) compound. Samples were sectioned at 10 mm. The sections were fixed in 4% paraformaldehyde for 15 min and permeabilized using 0.3% Triton X-100 for 20 min. Organoids were treated with 1% BSA/PBS for 1 h. After three additional PBS washes, samples were incubated overnight with primary antibodies at 4°C. Specimens were washed three times in PBS and incubated with the corresponding secondary antibodies at a 1:200 dilution for 1 h. Samples were mounted with mounting medium containing the nuclear counterstain DAPI. Immunofluorescence images were obtained by an inverted Olympus IX71 microscope. Antibodies are listed in Table 1. The study involving adult human lung tissues was reviewed and approved by the Medical Ethics Committee of Zunyi Medical University ((2022)1–017). The lung cancer donor treated at The Second Affiliated Hospital of Zunyi Medical University provided written informed consent to participate.

Construction of an Adenovirus Infection Model of Human Airway Organoids

Adenovirus Infection of Airway Organoids

For infection experiments, cells grown in RADA16-I hydrogels were incubated for 7 days in a 12-well or 96-well plate, as previously described. Then, the cells were inoculated with adenovirus-EGFP (3×10^6 copies viral nucleotides per well in 12-well/1×10^6 copies viral nucleotides per well in 96-well) for 24 h at 37°C. Afterward, the solution was removed, and airway organoid cultures were washed three times with PBS and covered with complete medium. Observations were carried out every day after infection.

Proliferation of Adenovirus and Cytopathy

Airway organoid cultures in 12-well plates were infected with adenovirus-EGFP as previously described. The EGFP reporter gene was used as a label to detect virus proliferation under direct fluorescence microscopy at 3, 6, and 9 dpi. At the same time points, cytopathy was observed by inverted phase contrast microscopy.

Table 1 Cells Marker Proteins Associated with Airway Tissue

Primary Antibodies	Dilution	Label Cell	Secondary Antibodies and Fluorescence
Rabbit Anti-Human VIM	1:100	Mesenchymal cells	AF488-labelled goat anti-mouse IgG (Green)
Mouse Anti-Human CD31	1:200	Vascular endothelial cells	AF 647-labelled goat anti-Rabbit IgG (Red)
Rabbit Anti-Human AQP5	1:100	Alveolar epithelial type-I cells	AF488-labelled goat anti-mouse IgG (Green)
SPC Conjugated Antibody	1:100	Alveolar epithelial type-II cells	Red
Rabbit Anti-Human CC10	1:100	Proximal airway epithelial cells	AF488-labelled goat anti-mouse IgG (Green)
Mouse Anti-Human KRT8	1:200	Luminal airway epithelial cells	AF 647-labelled goat anti-Rabbit IgG (Red)

Cell Viability and Cell Proliferation Assay in Adenovirus-Infected Airway Organoids

Adenovirus (1×10^6 copies viral nucleotides per well) was inoculated into the airway-organoid model after 7 d of culture, while the control group was not infected with adenovirus. Afterward, 20 μL of MTS reagent was added to the wells at 0, 4, 8, 20 days, the cell samples were incubated at 37°C for 2 h in the dark, and the absorbance was measured at 490 nm. Airway organoids were maintained under normal adenovirus-infected conditions as described above and collected at each time point. DNA density (μg/mL) was determined by fluorometric quantification of the DNA content using a DNA fluorescence assay kit according to the manufacturer's instructions (Invitrogen, molecular probes). For qualitative observations of cell proliferation, the gel-cell clumps were incubated in PBS containing 10 μg/mL propidium iodide (PI) to stain dead cells. An inverted Olympus IX71 fluorescence microscope was used to capture fluorescent signals.

TEM Observation of Adenovirus in Airway Organoids

Airway organoids cultured in 3D conditions in a 12-well plate were infected with adenovirus as previously described, and the gel-cell clumps were harvested at 8 dpi. The samples were then postfixed using 1% osmic acid at 4°C for 3 h, dehydrated through a graded series of alcohol, embedded in Spurr resin, and cut into ultrathin sections (thickness 70 nm). Specimens were then stained with uranyl acetate and lead citrate, and images were obtained using a JEM1230 TEM (JEOL, Japan) at an acceleration voltage of 80 kV.

DNA Extraction and Quantitative qPCR of Organoid-Cultured Adenovirus

Airway organoids in 96-well plates were infected with adenovirus (1×10^6 copies viral nucleotides per well), and the gel-cell clumps were harvested at 1, 3, 5, and 15 dpi and stored at −20°C. Subsequently, viral nucleic acids were extracted with a DNA/RNA extraction kit (Tiangen DP315) according to the manufacturer's protocol. qPCR systems were prepared using a BIO-RAD qPCR kit in accordance with the manufacturer's protocol. The primers used for detection were as follows: EGFP, 5′-TTCAAGATCCGCCAC-AACA-3′ and 5′- CGCTTCTCGTTGGGGTC-3′. The qPCR conditions were as follows: predenaturation at 95°C for 2 min, 39 cycles of denaturation at 95°C for 5 s, annealing at 60°C for 30s and a melting curve temperature between 65°C and 95°C. Negative (water) and positive (adenovirus standard samples) controls were established for each amplification. After the reaction was complete, the system automatically generated a standard curve and calculated the copy number of the complete viral genome in the corresponding samples.

Detection of Adenovirus Infectivity Produced in Airway Organoids

The gel-cell clumps in the supernatants were collected at 9 dpi (5×10^5 copies based on qPCR amplification quantification) and then used to infect 293T cells grown in 2D culture. The supernatants and cells of 2D culture were collected at 24, 48 and 72 hpi. Thereafter, viral DNA was extracted and amplified by qPCR.

Statistics

All statistical analyses were performed using SPSS18.0. Each data point represents the mean of at least three independent experiments. Data are represented as the mean value ± SD of a triplicate experiment. Independent sample *t*-tests were used for comparisons between the two groups, and a value of 0.05 was the significance threshold for all assays.

Results

Scaffold Characterization of RADA16-I

SEM was used to analyze the reticulated nanofiber structure of the RADA16-I Nanogel in solution (Figure 1). RADA16-I self-assembled in the presence of ions to form highly crosslinked nanofibers, and interwoven nanofiber networks were clearly observed. The fibers were uniform and long, crossed into a grid, and wound around each other into a three-dimensional network structure, similar to the structure of the ECM.

Cell Proliferation in 3D Culture

As shown in Figure 2A-I–C-I), HSAEC1-KT, HuLEC-5a and HELF cells in 2D culture all showed flat monolayer growth. However, in RADA16-I Nanogel 3D culture starting with a single cell, dense multicellular microspheres began to form on the third day of culture. The microspheres of HSAEC1-KT and HuLEC-5a cells were round (Figure 2A-II and B-II), and

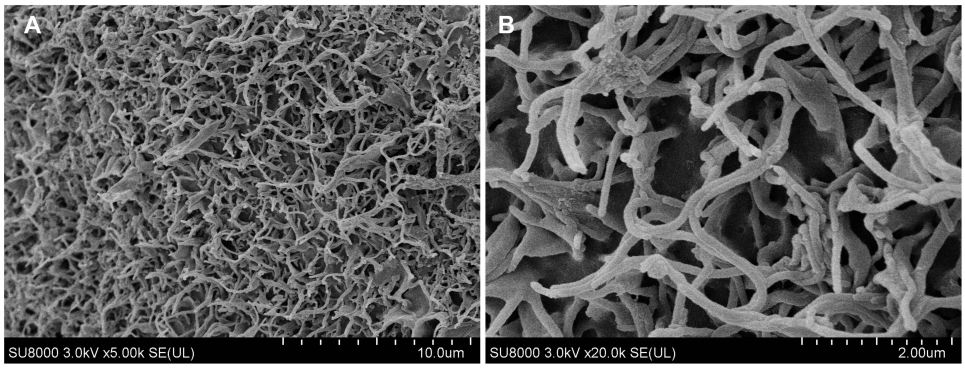

Figure 1 RADA16-I was evaluated by SEM and applied to 3D cell cultures. (**A**) and (**B**) are SEM images of RADA16-I peptide scaffold nanofibers, RADA16-I self-assembled to form crosslinked nanofiber grids, and its porosity was similar to that of the natural ECM.

branches appeared around the microspheres of HELF cells (Figure 2C-II). The microspheres of HSAEC1-KT, HuLEC-5a and HELF cells increased with prolonged culture time (Figure 2A-III–C-III), On the 7th day, the branches of the HELF cell microspheres were cross-linked with each other (Figure 2C-III). suggesting that the three kinds of cells could grow well in the RADA16-I Nanogel and that HELF cells had an aggregation function in the RADA16-I Nanogel.

Construction of the Airway Organoid Model

Morphological Observation

HSAEC1-KT, HuLEC-5a and HELF cells were cocultured in RADA16-I Nanogel. The ratio of the HSAEC1-KT: HuLEC-5a: HELF cell types was 10:7:2. Inverted microscopy showed that the cells were scattered on the first day (Figure 2D-I). With the extension of culture time, the cell groups gradually grew, connected with each other, and began to self-assemble. On the 7th day, the self-assembly was tubular (Figure 2D-II). On the 14th day of culture, the cell self-assembly showed a lumen-like structure, similar to the structure of the human airway (Figure 2D-III). However, HSAEC1-KT cells alone in 3D culture showed microsphere aggregation and no lumen-like structure (Figure 2E-I-III). Further observation of the growth of the cocultured cells by inverted phase contrast microscope and SEM showed that interconnected cells in the RADA16-I Nanogel grew in three dimensions and were closely connected with each other, which resembled the growth morphology of host cells in vivo (Figure 2F and G). TEM observation revealed that the cells were connected and communicated with each other (Figure 2H). It is suggested that RADA16-I Nanogel can not only provide an ECM-like microenvironment for cell growth but also promote the growth of mixed cell populations of HSAEC1-KT, HuLEC-5a and HELF to form an airway-like lumen structure.

Histological Observation

To further verify whether the airway-like lumen structure was hollow under an inverted microscope, airway-like cell masses cultured in RADA16-I Nanogel for 14 days were embedded in OCT and observed by H&E staining and phalloidin staining. The 3D results showed that HSAEC1-KT cells cultured alone gathered into dense cell clusters without lumen-like structures (Figure 3A-I and B-I). In contrast, the airway-like structure formed by the self-assembly of mixed cells was a hollow lumen, and a large number of cells were arranged and distributed around the lumen (Figure 3A-II and B-II), which is similar to the normal lung tissue structure (Figure 3A-III and B-III). These results suggest that HSAEC1-KT, HuLEC-5a and HELF cells cocultured at 10:7:2 in RADA16-I Nanogel can self-assemble to form a hollow airway-like structure, which is similar to normal human airway tissue.

Cell Viability, Proliferation and Growth

We then investigated the activity and proliferation of cells self-assembled into airway-like organs. Preliminary cell growth and viable cell fate were observed by green fluorescent Ca-AM staining and DNA quantitative analysis. The results of Ca-AM/PI staining showed that the HSAEC1-KT, HuLEC-5a and HELF cells had good cell activity with almost no dead cells, and the cell aggregation was similar to that of a small airway on the 6th day (Figure 4A). A tube-

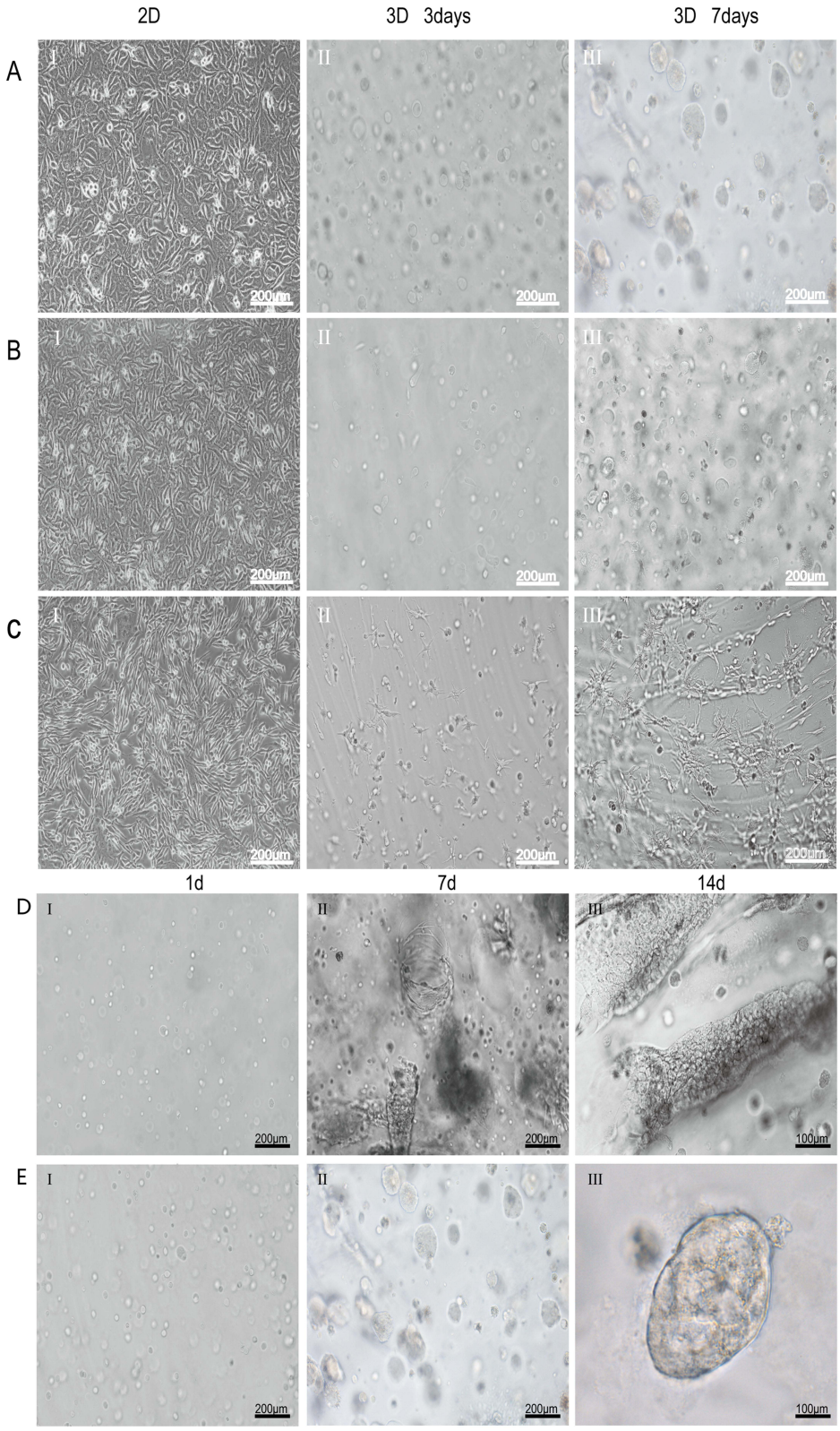

Figure 2 Continued.

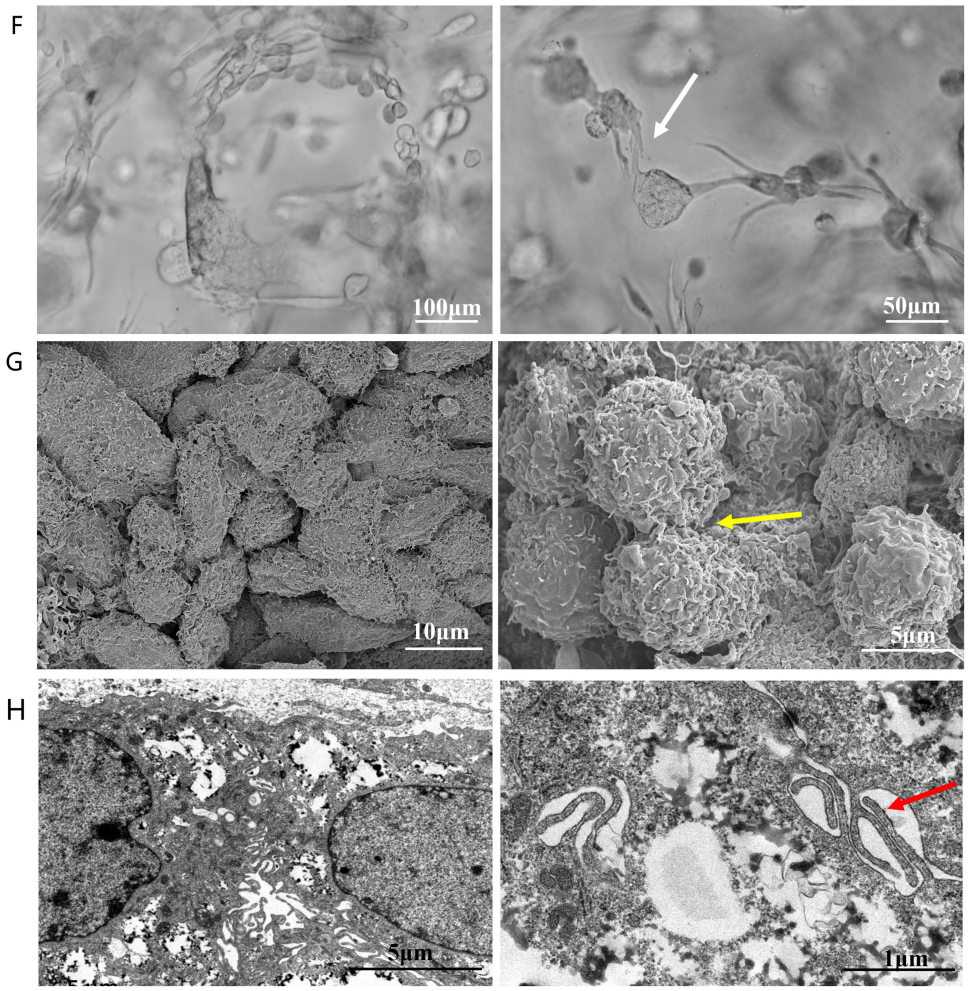

Figure 2 Growth and morphological characteristics of cells in 3D culture. (**A**–**C**) Phase-contrast images of HSAEC1-KT, HuLEC-5a and HELF cells cultured in 2D for 3 days and 3D conditions for 3 days and 7 days. In 2D culture, the cells grew in a flat monolayer. In 3D culture, the cells formed dense multicellular spheroids, and the cell spheres increased gradually over time. Branches and crosslinks appeared around the multicellular spheres cultured by HELF 3D culture (**D**). Phase-contrast images of HSAEC1-KT, HuLEC-5a and HELF cocultured in RADA16-I hydrogel at a ratio of 10:7:2 for 1 day, 7 days and 14 days. On the first day of culture, the cells were scattered and distributed; on the 7th day, the cells self-assembled and showed tubular growth; on the 14th day, the tracheal structure was formed (**E**). Phase-contrast images of HSAEC1-KT in RADA16-I hydrogel for 1 day, 7 days and 14 days. Multicellular spheroids appeared and gradually increased in size (**F**). Phase-contrast images of HSAEC1-KT, HuLEC-5a and HELF cocultured in RADA16-I hydrogel at a ratio of 10:7:2 for 7 days. These cells were self-assembled into tubes through mutual aggregation (**G**). SEM showed that the cells were connected to each other, the cells gathered together showed 3D growth, and the cells were closely connected (**H**). TEM observation showed that the cells were connected by pseudopods. Interconnected cells are indicated by the white arrow, three-dimensional cells are indicated by the yellow arrow, and pseudopods are indicated by the red arrow.

like structure was observed on the 12th day of culture. The cell activity was still good, and only a few dead cells were observed (Figure 4B). However, HSAEC1-KT cells cultured alone in 3D formed spherical or nearly spherical structures, and with extension of the culture time, the microspheres gradually expanded, no lumen-like structure was observed, and the cell activity remained good (Figure 4C and 4D). The proliferative activity of HSAEC1-KT, HuLEC-5a, and HELF cells 3D cultured individually and that of fixed cultured cells was detected by MTS. The results showed that the cells could proliferate well for a long time. The proliferative activity was maintained at a high level from 8 to 16 days and then decreased gradually (Figure 4E). DNA quantitative analysis showed that the cells continued to proliferate after 20 days (Figure 4F). The above results show that the cocultured cells can self-assemble to form an air-like structure and maintain proliferative activity for a long time.

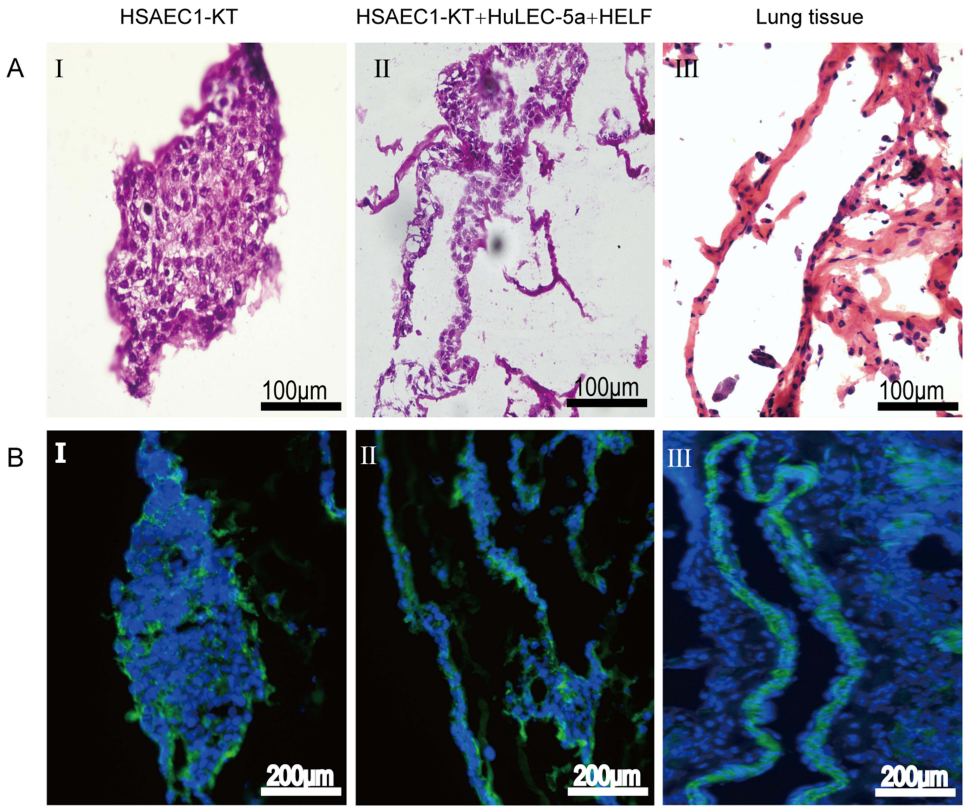

Figure 3 The morphology and structure of 3D cultured cells and normal lung tissues were observed by H&E staining and phalloidin staining. (**A**) H&E staining. (**B**) Phalloidin staining (**A**-I and **B**-I). Gel-cell clumps of HSAEC1-KT cells in RADA16-I were harvested on day 14 and then stained by frozen sectioning. The cells were clustered into dense cell masses without tubular structure (**A**-II and **B**-II). Gel-cell clumps of HSAEC1-KT, HuLEC-5a and HELF cocultured in RADA16-I at a ratio of 10:7:2 were harvested on day 14 and then stained by frozen sectioning. The cells self-assembled into a hollow tubular structure, and a large number of cells were arranged and distributed around the lumen (**A**-III and **B**-III). Human normal lung tissues were stained as frozen sections. The structure of the airway lumen was observed, and a large number of cells were arranged and distributed around the lumen. Green indicates F-actin, and blue indicates DAPI-stained cell nuclei.

Expression of Specific Labeled Proteins in Airway Organoids

To further clarify whether airway-like structures express airway tissue-specific labeled proteins, immunofluorescence staining was used to detect the expression of the mesenchymal cell marker protein VIM, the vascular endothelial cell marker protein CD31, the proximal airway epithelial cell marker protein CC10, the distal lung alveolar epithelial cell type I (AECI) and type II (AECII) marker proteins AQP5 and SPC, and the luminal marker protein KRT8, and the results were compared with those in normal lung tissue. HSAEC1-KT, HuLEC-5a and HELF cells were cocultured in RADA16-I Nanogel at a ratio of 10:7:2. On the 14th day, OCT-embedded frozen sections were stained with immunofluorescence. The results showed that the expression of VIM (Figure 5A-I), CD31 (Figure 5A-II), AQP (Figure 5B-I), SPC (Figure 5B-II), CC10 (Figure 5C-I), and KRT8 (Figure 5C-II) was similar to that in normal lung tissue structure (Figure 5D–F). The airway epithelial marker protein KRT8 is related to airway lumen formation. The results showed that KRT8 was persistently and stably expressed in the lumen on the 14th and 21st days of culture (Figure 5G and H). Epithelial cell clusters self-assembled into tubular structures of varying shapes and sizes. These results suggest that the cocultured cells can self-assemble to form airway-like organs and express specific biomarkers related to airway tissue.

Construction of an Adenoviral Infection Model of Airway Organoids

Viral Proliferation in Airway Organoids

We cocultured HSAEC1-KT cells at a ratio of 10:7:2 with HuLEC-5a and HELF cells in RADA16-I Nanogel, and the tubular structure was formed on the 7th day and infected with adenovirus-EGFP. The successfully infected cells showed a green fluorescence signal under a fluorescence inverted microscope. As shown in Figure 6A, green fluorescent cells were observed in the airway organoids at 3 dpi, but the fluorescence intensity was very weak. Thereafter, the number of

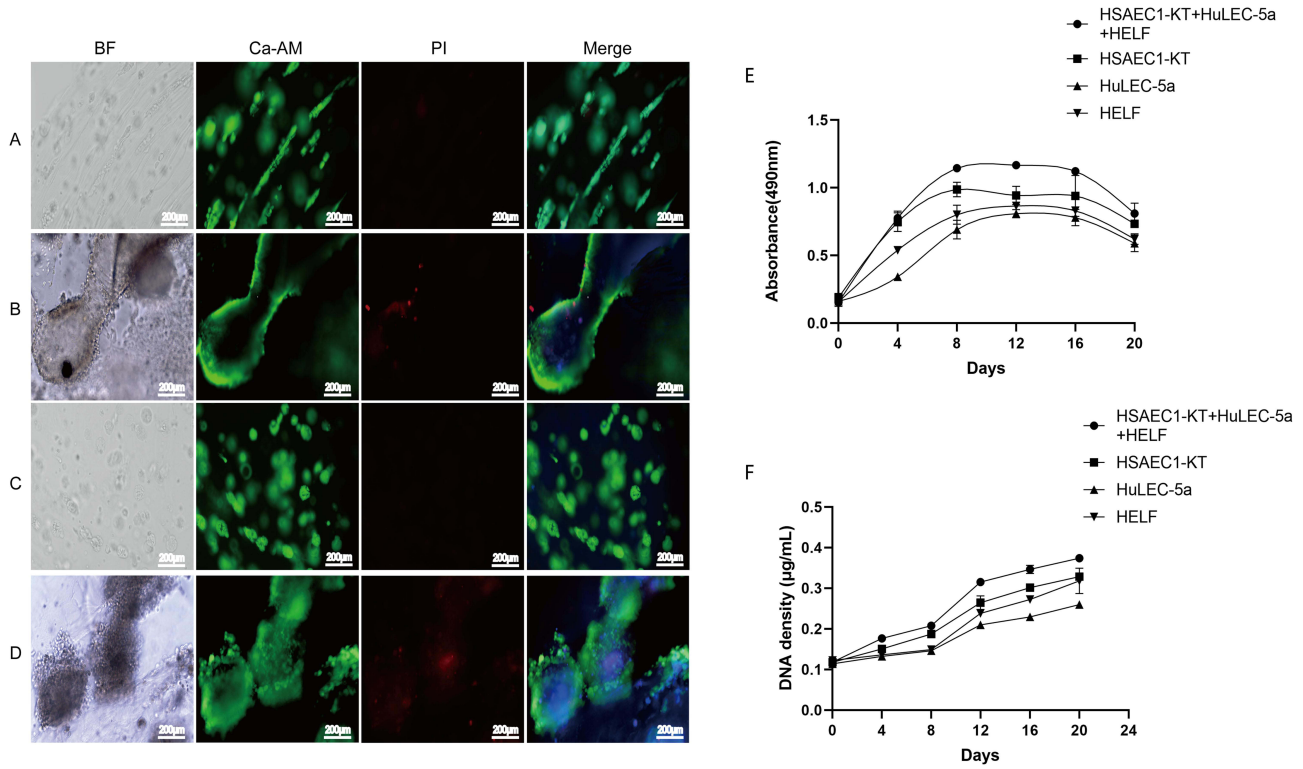

Figure 4 Proliferation and activity analysis of cells in RADA16-I hydrogels. (**A** and **B**). Morphology and activity of HSAEC1-KT, HuLEC-5a and HELF cocultured in RADA16-I hydrogels at a ratio of 10:7:2 for 6 and 12 days. With the extension of culture time, the self-assembly of the cell population showed growth of the airway structure, and the cell activity was good (**C** and **D**). Morphology and activity of HSAEC1-KT in RADA16-I hydrogels for day 6 and day 12. The cells gathered as dense microspheres, and the cell activity was good. Ca-AM staining in green shows the live cells, PI staining in red shows the dead cells, and DAPI staining in blue shows the cell nucleus (**E**). The proliferative activity curves of HSAEC1-KT, HuLEC-5a, HELF and cocultured cells in RADA16-I hydrogels were detected by MTS. All the cells could grow in RADA16-I hydrogels for a long time with good proliferative activity. The proliferative activity remained high at 8–16 days and then declined gradually. Each data point represents the mean of at least three independent experiments (**F**). The viable cell proliferation curves of HSAEC1-KT, HuLEC-5a, HELF and cocultured cells in RADA16-I hydrogel were calculated from DNA quantitative analysis. All the cells proliferated continuously in the RADA16-I hydrogel. Each data point represents the mean of at least three independent experiments.

fluorescent cells and the fluorescence intensity increased gradually from the edge of the gel, reaching a maximum at 9 dpi. With the extension of infection time, the number of round and scattered cells in the Nanogel gradually increased (Figure 6B). TEM scans were performed to further observe the adenovirus particles in the cells of infected airway organoids, and at 8 dpi, a small number of virions with diameters of 60–90 nm were observed in the cytoplasm (Figure 7). These results showed that adenovirus could infect airway organoids and cause cytopathic effects.

Analysis of Cell Viability and Proliferation

The effect of adenovirus infection on the proliferation and activity of airway organoids was observed. HSAEC1-KT, HuLEC-5a and HELF cells were cocultured in RADA16-I Nanogel at 10:7:2 and infected with adenovirus on the 7th day. PI staining, the MTS method and DNA quantitative analysis were used to detect the cell activity and proliferation of airway organoids after adenovirus infection. PI staining showed that the red fluorescence signal of airway organoids was strong at 9 dpi, and the cells were obviously round and scattered in the bright-field image (Figure 6C), indicating that adenovirus infection and proliferation could cause cytopathic changes and even death in airway organoids. The cell activity of airway organoids infected with adenovirus was detected by MTS. The results showed that the cell activity of airway organoids in the infected group was lower than that in the uninfected group ($P<0.01$) from 12 to 20 days of culture (4–12 dpi) (Figure 6D). DNA quantitative analysis showed that the cell proliferation in the infected group was lower than that in the uninfected group ($P<0.01$) after 12 to 20 days of culture (4–12 dpi) (Figure 6E). The above results suggested that the cells of airway organoids showed pathological changes and that their proliferation and activity decreased after adenovirus infection.

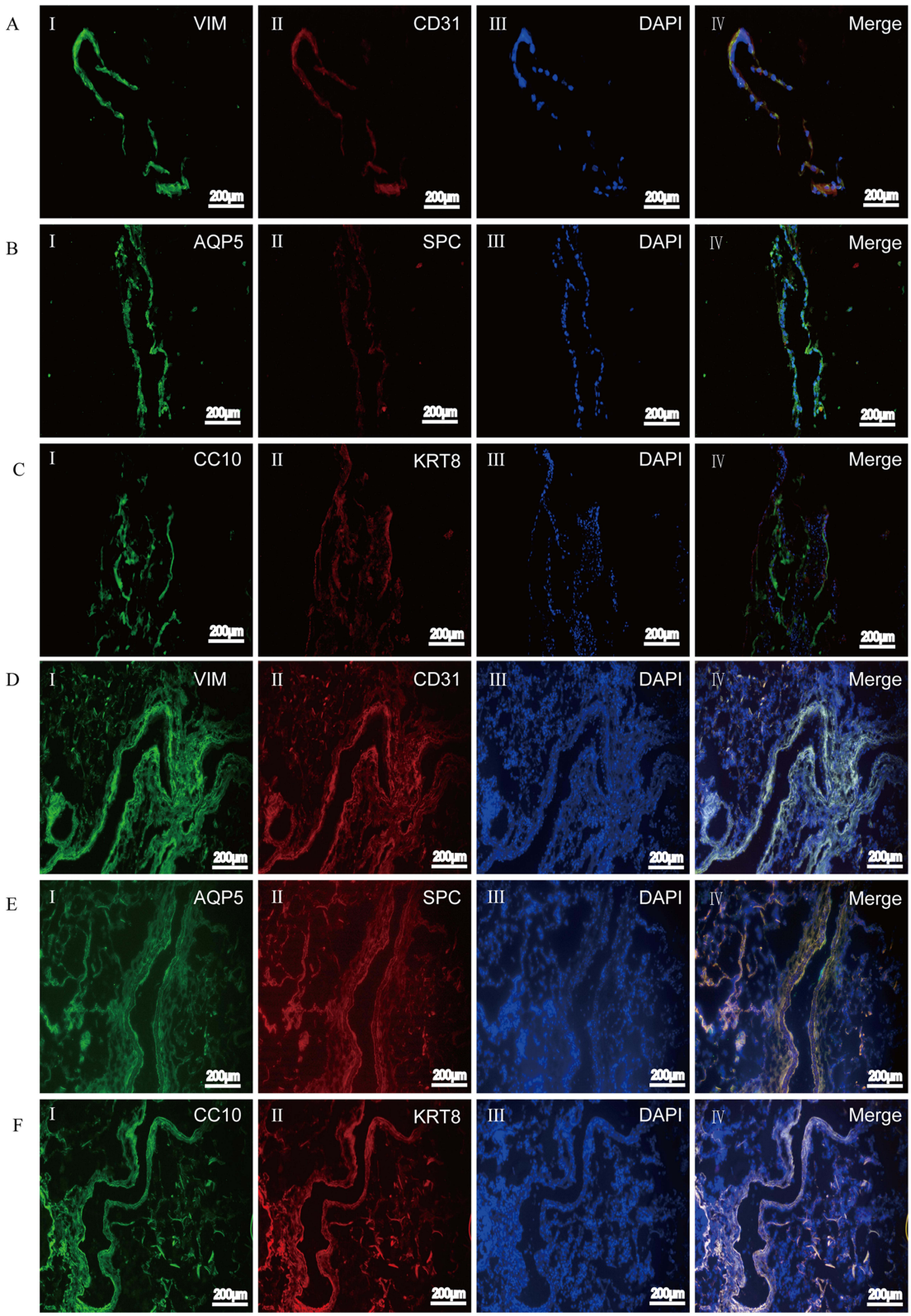

Figure 5 Continued.

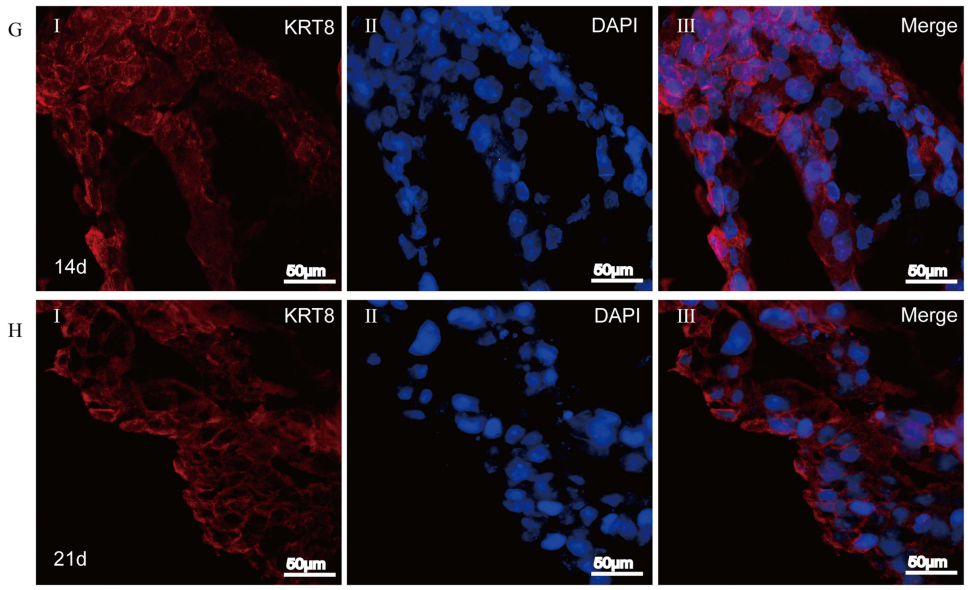

Figure 5 Self-organization of cells within airway organoids and the expression of specific marker proteins. (**A**–**C** and **G**) Frozen sections of airway organoids cultured for 14 days. (**H**) Frozen sections of airway organoids cultured for 21 days. (**D**–**F**) Frozen sections of normal lung tissue. mesenchymal cells VIM (green, **A**-I), vascular endothelial cells CD31 (red, **A**-II), and proximal airway epithelial cells CC10 (green, **C**-I) clustered together and then differentiated into distal alveolar epithelial cells AECI AQP5 (green, **B**-I) and AECII SPC (red, **B**-II) formed the lumen structure of the airway sample and stably and continuously expressed the lumen airway epithelial marker protein KRT8 (red, **C**-II, **G**-I and **H**-I). Airway organoid cell arrangement and labeled protein expression were similar to those of normal human lung tissue (**D**–**H**). DAPI (blue, showing nucleus).

Characteristics of Adenovirus Replication in Airway Organoids

We next monitored viral DNA at different time points after infection by qPCR. The results of qPCR detection showed that the viral load of airway organoids infected by adenovirus began to increase significantly at 3 dpi and proliferated rapidly. The viral load reached 5.15×10^5 copies/mL at 9 dpi and then decreased rapidly, and almost no viral nucleic acid was detected at 15 dpi. To determine whether the inoculated adenovirus remained in the RADA16-I Nanogel, resulting in incorrect qPCR detection, adenovirus infection and nucleic acid detection were also performed on the cell-free RADA16-I Nanogel. The results showed that a large number of viruses in the RADA16-I Nanogel were not detected in the absence of cells (Figure 8A). The adenovirus amplified from RADA16-1 Nanogel successfully infected 2D cultured 293T cells and proliferated continuously, and the proliferation trend was consistent with that of the 2D adenovirus standard infection group (Figure 8B). This shows that adenoviruses can infect airway organoids and be amplified.

Discussion

Organoid technology has developed rapidly in recent years, and organoids are considered an ideal model for the in-depth exploration of virus pathogenesis and host–virus interactions, antiviral drug screening, and vaccine research and development.[29–31] Currently, hESCs or hiPSCs are most commonly used for organoid construction, but the culture process requires the addition of multiple growth factors to promote the induction and differentiation of organoids. The culture conditions are complex, the cost is high, and there are ethical problems. Moreover, there are many uncertain factors affecting the experimental results. These problems also exist in using normal tissue or tumor tissue to induce differentiation to construct organoids. However, using cell lines to construct organoids is relatively simple and inexpensive. In this study, human lung-derived cell lines (HSAEC1-KT, HuLEC-5a, HELF) were used to construct airway organoids. The growth time of the three kinds of cells was limited under two-dimensional culture conditions, and the cells were stretched flat. When the three kinds of cells were cultured separately in RADA16-I hydrogel, the cells grew like microspheres. The microspheres could maintain growth for a longer time without the formation of a tracheal cavity structure. When the three cell types were cocultured in RADA16-I Nanogel at a ratio of HSAEC1-KT: HuLEC-5a: HELF=10:7:2, the cells could form tracheal structures more similar to the airways through self-assembly, and the cells

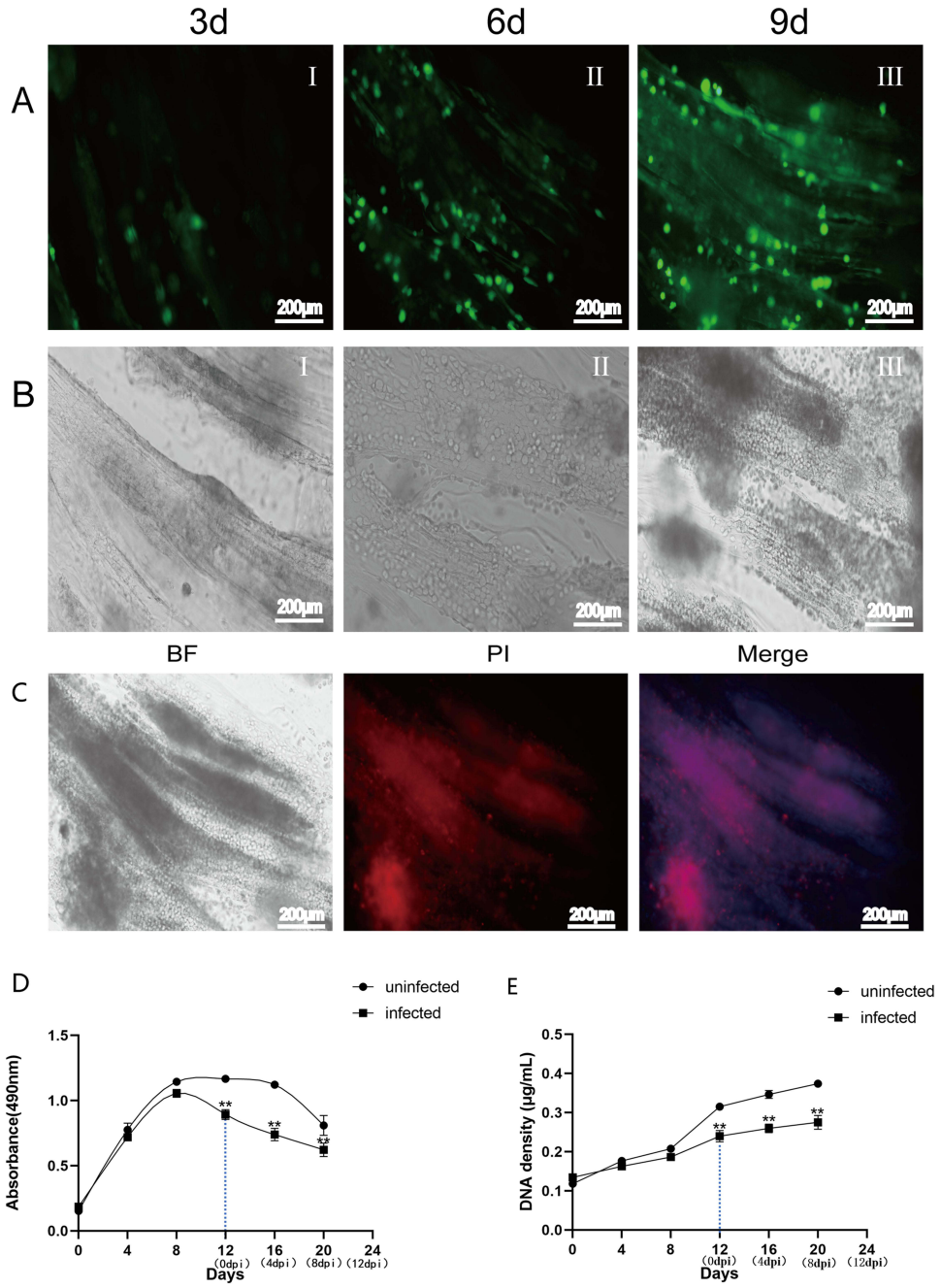

Figure 6 Growth and proliferation activity of airway organoids after adenovirus infection. (**A**). Fluorescence microscopy observation of airway organoids at 3 dpi, 6 dpi and 9 dpi. Green fluorescent cells were observed at 3 dpi, and the number of fluorescent cells and the fluorescence intensity increased gradually from the edge of the gel, peaking at 9 dpi (**B**). Inverted microscope observation of airway organoids at 3 dpi, 6 dpi and 9 dpi. With the extension of infection time, the cells in airway organoids became round and scattered. Adenovirus (Adenovirus-EGFP, green fluorescence) (**C**). PI staining observation of airway organoids at 9 dpi. The red fluorescence signal was strong, there were more dead cells, and the lesions of cells were visible under the bright field view (**D**). The proliferative activity curves of airway organoids after adenovirus infection were obtained by MTS. The cell activity of airway organoids in the infected group was significantly lower than that in the uninfected group at 12 to 20 days after culture (4 dpi to 12 dpi). Each data point represents the mean of at least three independent experiments (**E**). The viable cell proliferation curves of airway organoids after adenovirus infection were calculated from DNA quantification. The cell proliferation of airway organoids in the infected group was significantly lower than that in the uninfected group at 12 to 20 days after culture (4 dpi to 12 dpi). Each data point represents the mean of at least three independent experiments; PI (red, indicating dead cells) and DAPI (blue, indicating nuclei). The dotted line indicates the onset of infection;**Compared with the uninfected group, $P < 0.01$.

could maintain their activity and proliferation for a long time. At the same time, the expression of proximal airway epithelial cell marker protein (CC10), distal alveolar epithelial marker protein (AQP5, SPC), vascular endothelial cell marker protein (CD31), mesenchymal cell marker protein (VIM), and lumen formation-related epithelial marker protein (KRT8) was detected, which shows that the cells differentiate into distal lung tissue through coculture and self-assembly.

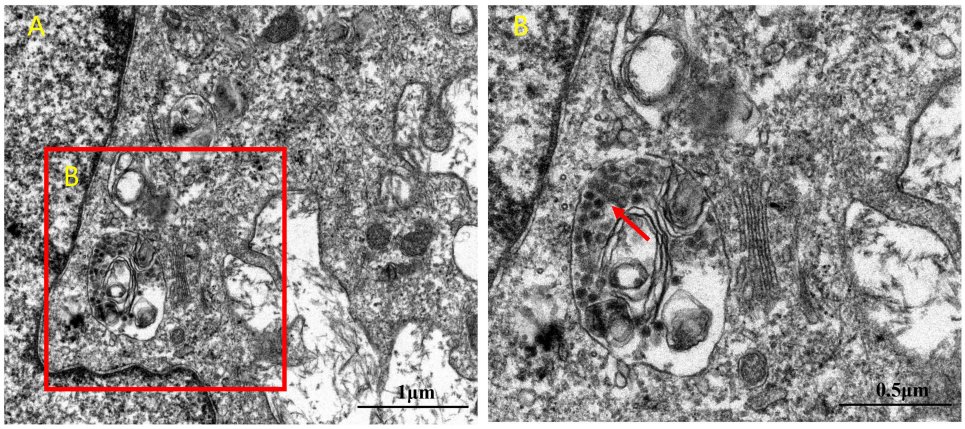

Figure 7 TEM analysis of adenovirus virions in airway organoids. (**A**). The nucleus and cytoplasmic region of the cells in the airway organoids (**B**). The region where adenovirus particles appear in the cytoplasm. Virus-like particles are indicated by the red arrows.

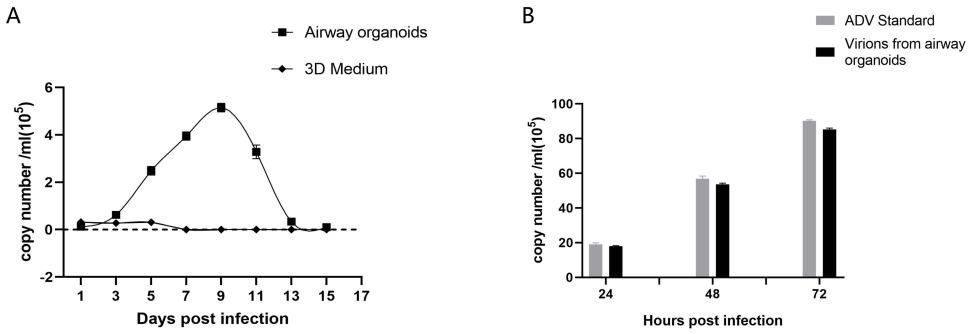

Figure 8 qPCR measurement of adenovirus proliferation in airway organoids. (**A**). Adenovirus proliferation in airway organoids was measured by qPCR. "airway organoids" indicates adenovirus amplification in airway organoids; "3D medium" indicates adenovirus amplification in RADA16-I hydrogel without cells (**B**). The infectivity of airway organoid-amplified virions was measured by qPCR. "ADV Standard" indicates standard adenovirus amplification in 2D culture; 'virions form airway organoids' indicates airway organoid-generated adenovirus virions (5×10^5 copies based on qPCR amplification quantification) in 2D culture. Airway organoid-generated adenovirus virions were present in airway organoid supernatants harvested at 9 dpi. Each data point represents the mean of at least three independent experiments.

This is similar to the results reported by Tan et al.[13] This suggests that organoids similar to airway tissue in vivo can be successfully constructed by using human lung-derived cell lines and cocultures in certain proportions.

With the development of biotechnology, a variety of biological materials have been used in 3D cell culture. As a kind of biological material, nano-self-assembled peptides have unique amino acid sequences and easily self-assemble into a nanonetwork fiber structure with a water content of more than 99% in physiological salt solution by using existing molecular components in nature. Among them, RADA16-I is a commonly used scaffold for cell culture, possibly because of its amino acid sequence design. The sequence RAD (arginine-alanine-aspartic acid) is similar to the sequence of the RGD (arginine-glycine-aspartic acid) polypeptide, the ligand binding site of integrin on the cell membrane.[32] It provides a microenvironment similar to the natural ECM in which cells can adhere to hydrogels and grow. In this study, RADA16-I was used as a scaffold for cell culture, which provided a microenvironment similar to that in vivo for cell growth, which was conducive to the growth and aggregation of cell populations. At the same time, human embryonic lung fibroblasts (HELFs) were selected in the culture, which had an agglutinative effect. In the RADA16-I hydrogel, the cells formed long pseudopods and grew like branches, which made the connections between cells tight, conducive to communication between different cells, and thus promoted the self-assembly of cells to form airway organoids. In this study, no additional growth factors were added in the culture process of constructing airway organoids, and normal culture conditions were adopted. Compared with organoid construction induced by stem cell differentiation, this method has the advantages of simplicity, low culture cost and a short culture cycle, which is more conducive to repeated experiments

and batch research. This approach also provides an experimental basis for the use of nano-self-assembled peptide hydrogels to construct a bionic model of human organoids.

Adenoviruses have a diameter of 60~90 nm, while the fiber mesh size formed by RADA16-I self-assembly is approximately 5~200 nm. Previous studies have demonstrated that the virus can infect 293T cells through scaffold pores. In this study, three human lung cell lines were cocultured until the 7th day. When the tracheal structure of the airway sample was observed, adenovirus was added to construct the infection model. The qPCR results showed that the amount of adenovirus increased logarithmically at 3 dpi and peaked at 9 dpi. The rapid proliferation time is consistent with the incubation period of clinical adenovirus infection, which shows that this model can accurately simulate clinical adenovirus infection. At the same time, cell proliferation activity decreased significantly from 4 dpi, which may be because adenoviruses are nonenveloped viruses, which lead to damage and rupture of host cells after massive replication and the release of progeny viruses. Airway epithelial cells are the main constituent cells of airway tissue and are sensitive cells to adenovirus infection. These airway organoids can simulate the characteristics of internal organs composed of various cells, simulate the morphological structure and phenotype characteristics of airway tissue, and reproduce the process of viral infection. However, in the traditional 2D culture model, after the virus infects monolayer cells, the cells usually exhibit rapid rounding, shedding, necrosis and other phenomena: the virus cannot proliferate repeatedly, and the infection is maintained for a short time and unable to reproduce the infection process in vivo. In this study, the adenovirus-infected airway organoid model maintained a long proliferation time, and the amplified progeny virus was infectious, similar to the viral behavior during in vivo infection. This model can provide a more reliable experimental platform for adenovirus isolation and culture, pathogenic mechanism research and antiviral drug development.

In this study, airway organoids were successfully constructed using RADA16-I hydrogel as a scaffold, and an adenovirus infection model of airway organoids was established in vitro on this basis. However, there are some limitations. First, this study confirmed that adenovirus can maintain long-term proliferation in these airway organoids, but whether it can be used as an infection model for other respiratory viruses needs further study. Second, the self-assembly ability of airway organoids constructed by cell lines from different sources is random, so the conditions need to be further optimized to establish a stable and large-scale bionic organoid model, and whether the airway organoids constructed by these cell lines can truly replace the physiological states of different individuals also needs to be further discussed. Third, the internal organs have a vascular system. In this study, human pulmonary microvascular endothelial cells (HuLEC-5a) were selected for the construction of blood vessels, but no angiogenesis was observed, which needs to be further studied by coculture with cells with vascular differentiation potential. In conclusion, three human lung-derived cell lines (HSAEC1-KT, HuLEC-5a, HELF) in RADA16-I hydrogel showed strong self-assembly ability and certain differentiation potential and could form airway-like morphology. However, these airway organoids still differ from normal human airway tissue due to the lack of a complete system, such as the circulatory system, immune system and nervous system, so it is necessary to further explore the construction of a coculture system with endothelial, neuron, immune and other lineages of cells, which is similar to the current status of reported organoid research.[33,34] The body is a complex environment where multiple organs and systems coexist. Viruses infect the body, grow in the body, and cause a series of processes, such as the occurrence and development of diseases, which involve not only a single organ system but also complex pathophysiological processes involving multiple organs and systems. Some scholars[35] have combined organoid culture technology with chip technology to build an organoid integrated system on a chip platform for drug screening research. Organ-on-A-chip systems can connect various organoids to each other to make up for the isolated communication of a single organoid, which may have epoch-making significance for the prevention, diagnosis and treatment of viral diseases.

Conclusion

An airway-organoid model for adenovirus infection with three human lung-derived cell lines was successfully constructed in vitro based on nano-self-assembling peptide RADA16-I hydrogels. The model has the potential to be exploited as a novel research method for adenovirus isolation and culture, pathogenesis research, and antiviral drug screening. This model can be expected to be used to explore new targets for the diagnosis and treatment of respiratory virus infection and explore new strategies for diagnosis, treatment and functional therapy.

Abbreviations

3D, three-dimensional; 2D, two-dimensional; ECM, extracellular matrix; TEM, transmission electron microscope; SEM, scanning electron microscope; Ca-Am, calcein-AM; dpi, days post infection; EGFP, enhanced green fluorescent protein; qPCR, real-time fluorescent quantitative PCR; Nanogel, nano-self-assembling peptide hydrogel; HSAEC1-KT, human small airway epithelial cells; HuLEC-5a, human lung microvascular endothelial cells; HELF, and human embryonic lung fibroblasts; hESCs, human embryonic stem cells; hiPSCs, human induced pluripotent stem cells; hASCs, human adult stem cells.

Data Sharing Statement

All relevant data are available from the authors upon request.

Ethics Approval

Medical Ethics Committee of Zunyi Medical University, ((2022)1-017), this study complies with the Declaration of Helsinki.

Author Contributions

All authors made a significant contribution to the work reported, whether in the conception, study design, execution, acquisition, analysis and interpretation of data or in all these areas; took part in drafting, revising or critically reviewing the article; gave final approval of the version to be published; have agreed on the journal to which the article has been submitted; and agree to be accountable for all aspects of the work.

Funding

This work was supported by the National Natural Science Foundation of China (81660340); the Basic Research Program Project (Natural Science) of Guizhou Province (Qian ke he ji chu-ZK [2022]584); the Construction Project of the Educational Department of Guizhou (Grant No. [2022]027); and the National College Students Innovation and Entrepreneurship Training Program (202210661233).

Disclosure

Yun-E Xu and Di-Shu Ao are co-first authors for this study. The authors declare no conflicts of interest in this work.

References

1. Louz D, Bergmans HE, Loos BP, et al. Animal models in virus research: their utility and limitations. *Crit Rev Microbiol*. 2013;39(4):325–361. doi:10.3109/1040841X.2012.711740
2. Griffith LG, Swartz MA. Capturing complex 3D tissue physiology in vitro. *Nat Rev Mol Cell Biol*. 2006;7(3):211–224. doi:10.1038/nrm1858
3. Rosellini A, Freer G, Quaranta P, et al. Enhanced in vitro virus expression using 3- dimensional cell culture spheroids for infection. *J Virol Methods*. 2019;265:99–104. doi:10.1016/j.jviromet.2018.12.017
4. Imle A, Kumberger P, Schnellbacher ND, et al. Experimental and computational analyses reveal that environmental restrictions shape HIV-1 spread in 3D cultures. *Nat Commun*. 2019;10(1):2144. doi:10.1038/s41467-019-09879-3
5. Koban R, Lam T, Schwarz F, et al. Simplified bioprinting-based 3D cell culture infection models for virus detection. *Viruses*. 2020;12(11):1298. doi:10.3390/v12111298
6. Pei R, Feng J, Zhang Y, et al. Host metabolism dysregulation and cell tropism identification in human airway and alveolar organoids upon SARS-CoV-2 infection. *Protein Cell*. 2021;12(9):717–733. doi:10.1007/s13238-020-00811-w
7. Dubich T, Dittrich A, Bousset K, et al. 3D culture conditions support Kaposi's sarcoma herpesvirus (KSHV) maintenance and viral spread in endothelial cells. *J Mol Med*. 2021;99(3):425–438. doi:10.1007/s00109-020-02020-8
8. Chen YX, Xie GC, Pan D, et al. Three-dimensional culture of human airway epithelium in matrigel for evaluation of human rhinovirus c and bocavirus infections. *Biomed Environ Sci*. 2018;31(2):136–145. doi:10.3967/bes2018.016
9. Li Z, Yue M, Liu Y, et al. Advances of engineered hydrogel organoids within the stem cell field: a systematic review. *Gels*. 2022;8(6):379. doi:10.3390/gels8060379
10. Tang XY, Wu S, Wang D, et al. Human organoids in basic research and clinical applications. *Signal Transduct Target Ther*. 2022;7(1):168. doi:10.1038/s41392-022-01024-9
11. Ogundipe VML, Groen AH, Hosper N, et al. Generation and differentiation of adult tissue-derived human thyroid organoids. *Stem Cell Rep*. 2021;16(4):913–925. doi:10.1016/j.stemcr.2021.02.011

12. Tao J, Calvisi DF, Ranganathan S, et al. Activation of beta-catenin and Yap1 in human hepatoblastoma and induction of hepatocarcinogenesis in mice. *Gastroenterology*. 2014;147(3):690–701. doi:10.1053/j.gastro.2014.05.004
13. Tan Q, Choi KM, Sicard D, et al. Human airway organoid engineering as a step toward lung regeneration and disease modeling. *Biomaterials*. 2017;113:118–132. doi:10.1016/j.biomaterials.2016.10.046
14. Wilkinson DC, Alva-Ornelas JA, Sucre JM, et al. Development of a three-dimensional bioengineering technology to generate lung tissue for personalized disease modeling. *Stem Cells Transl Med*. 2017;6(2):622–633. doi:10.5966/sctm.2016-0192
15. Ramani S, Crawford SE, Blutt SE, et al. Human organoid cultures: transformative new tools for human virus studies. *Curr Opin Virol*. 2018;29:79–86. doi:10.1016/j.coviro.2018.04.001
16. Porotto M, Ferren M, Chen YW, et al. Authentic modeling of human respiratory virus infection in human pluripotent stem cell-derived lung organoids. *mBio*. 2019;10(3):e00723–19. doi:10.1128/mBio.00723-19
17. Salahudeen AA, Choi SS, Rustagi A, et al. Progenitor identification and SARS-CoV-2 infection in human distal lung organoids. *Nature*. 2020;588 (7839):670–675. doi:10.1038/s41586-020-3014-1
18. Depla JA, Mulder LA, De Sa RV, et al. Human brain organoids as models for central nervous system viral infection. *Viruses*. 2022;14(3):634. doi:10.3390/v14030634
19. Louz D, Bergmans HE, Loos BP, et al. Animal models in virus research: their utility and limitations. *Crit Rev Microbiol*. 2013;39(4):325–361. doi:10.3109/1040841X.2012.711740
20. Zhao X, Zhang S. Fabrication of molecular materials using peptide construction motifs. *Trends Biotechnol*. 2004;22(9):470–476. doi:10.1016/j.tibtech.2004.07.011
21. Yokoi H, Kinoshita T, Zhang S. Dynamic reassembly of peptide RADA16 nanofiber scaffold. *Proc Natl Acad Sci USA*. 2005;102(24):8414–8419. doi:10.1073/pnas.0407843102
22. Wang X, Wang J, Guo L, et al. Self-assembling peptide hydrogel scaffolds support stem cell-based hair follicle regeneration. *Nanomedicine*. 2016;12(7):2115–2125. doi:10.1016/j.nano.2016.05.021
23. He B, Ou Y, Chen S, et al. Designer bFGF-incorporated d-form self-assembly peptide nanofiber scaffolds to promote bone repair. *Mater Sci Eng C Mater Biol Appl*. 2017;74:451–458. doi:10.1016/j.msec.2016.12.042
24. Liu J, Song H, Zhang L, et al. Self-assembly-peptide hydrogels as tissue-engineering scaffolds for three-dimensional culture of chondrocytes in vitro. *Macromol Biosci*. 2010;10(10):1164–1170. doi:10.1002/mabi.200900450
25. Song H, Han YZ, Cai GH, et al. The effects of self-assembling peptide RADA16 hydrogel on malignant phenotype of human hepatocellular carcinoma cell. *Int J Clin Exp Med*. 2015;8(9):14906–14915.
26. Song H, Cai GH, Liang J, et al. Three-dimensional culture and clinical drug responses of a highly metastatic human ovarian cancer HO-8910PM cells in nanofibrous microenvironments of three hydrogel biomaterials. *J Nanobiotechnology*. 2020;18(1):90. doi:10.1186/s12951-020-00646-x
27. Ao DS, Gao LY, Gu JH, et al. Study on adenovirus infection in vitro with nanoself-assembling peptide as scaffolds for 3D culture. *Int J Nanomed*. 2020;15:6327–6338. doi:10.2147/IJN.S239395
28. Ao DS, Xu YE, Xin S, et al. Establishing a three-dimensional culture model of adenovirus using nanoself-assembling peptide KLD-12 hydrogels as scaffolds to evaluate the antiviral effects of IFNα2b. *Mater Express*. 2022;12(3):487–497. doi:10.1166/mex.2022.2164
29. Zou WY, Blutt SE, Crawford SE, et al. Human intestinal enteroids: new models to study gastrointestinal virus infections. *Methods Mol Biol*. 2019;1576:229–247. doi:10.1007/7651_2017_1
30. Costantini V, Morantz EK, Browne H, et al. Human norovirus replication in human intestinal enteroids as model to evaluate virus inactivation. *Emerg Infect Dis*. 2018;24(8):1453–1464. doi:10.3201/eid2408.180126
31. Saxena K, Simon LM, Zeng XL, et al. A paradox of transcriptional and functional innate interferon responses of human intestinal enteroids to enteric virus infection. *Proc Natl Acad Sci USA*. 2017;114(4):E570–E579. doi:10.1073/pnas.1615422114
32. Masuko T, Iwasaki N, Yamane S, et al. Chitosan-RGDSGGC conjugate as a scaffold material for musculoskeletal tissue engineering. *Biomaterials*. 2005;26(26):5339–5347. doi:10.1016/j.biomaterials.2005.01.062
33. Takebe T, Sekine K, Enomura M, et al. Vascularized and functional human liver from an iPSC-derived organ bud transplant. *Nature*. 2013;499 (7459):481–484. doi:10.1038/nature12271
34. Watson CL, Mahe MM, Munera J, et al. An in vivo model of human small intestine using pluripotent stem cells. *Nat Med*. 2014;20(11):1310–1314. doi:10.1038/nm.3737
35. Rajan SAP, Aleman J, Wan M, et al. Probing prodrug metabolism and reciprocal toxicity with an integrated and humanized multi-tissue organ-on-A-chip platform. *Acta Biomater*. 2020;106:124–135. doi:10.1016/j.actbio.2020.02.015